

Bioimaging for the monitoring of the *in vivo* distribution of infused mesenchymal stem cells in a mouse model of the graft-versus-host reaction

Sun-Young Joo*, Kyung-Ah Cho*, Yun-Jae Jung[†], Han-seong Kim[‡], Seong-Yeol Park^{||}, Yong-Bock Choi^{||}, Kyung-man Hong^{||}, So-Youn Woo*, Ju-Young Seoh* and Kyung-Ha Ryu^{1†}

* Department of Microbiology, Ewha Womans University School of Medicine, Ewha Medical Research Center, Seoul, South Korea

[†] Department of Pediatrics, Ewha Womans University School of Medicine, Ewha Medical Research Center, Seoul, South Korea

[‡] Department of Microbiology, Gachon Medical School, Incheon, South Korea

[§] Department of Pathology, Inje University Ilsan Paik Hospital, Ilsan, South Korea

^{||} Cancer Experimental Resources Branch, National Cancer Center, Ilsan, South Korea

Abstract

Cell therapy using MSCs (mesenchymal stem cells) might be effective treatment for refractory GVHD (graft-versus-host disease). However, the fate and distribution of MSCs after transplantation remains unclear. In this study, an animal model was developed to monitor the dynamic distribution of MSCs in mice with GVHD. A GVHD mouse model was established by transplanting C57BL/6 donor bone marrow cells and C57BL/6 EGFP (enhanced green fluorescent protein) splenocytes into lethally irradiated BALB/c nude recipient mice. Donor MSCs were obtained from MHC-identical C57BL/6 RFP (red fluorescent protein) mice and infused into the recipient mice on the same transplantation day. *In vivo* movement of the donor splenocytes (EGFP) and MSCs (RFP) were evaluated by measuring the biofluorescence (IVIS–Xenogen system). Donor splenocytes and MSCs reached the lungs first, and then the gastrointestinal tract, lymph nodes and skin, in that order; the transit time and localization site of these cells were very similar. In the recipient mouse with GVHD, the number of detectable cells declined with time, as assessed by biofluorescence imaging and confirmed by RT (real-time)-PCR. This bioimaging system might be useful for preclinical testing and the design of therapeutic strategies for monitoring the dynamic distribution of MSCs with GVHD.

Keywords: bioimaging; GVHD; mesenchymal stem cell

1. Introduction

Allogeneic HSCT (haematopoietic stem cell transplantation) is an established effective treatment for haematological malignancies and immunodeficiencies. This therapy includes the elimination of the haematopoietic compartment by irradiation and high-dose chemotherapy, which is followed by the reconstitution of the haematopoietic system by donor haematopoietic stem cells (Thomas et al., 1975).

However, the transplants also contain mature T cells that can induce GVHD (graft-versus-host disease), a major source of morbidity and mortality following allogeneic HSCT (Blazar et al., 1997). Donor T cells are strongly activated after the recognition of alloantigens of the recipient antigen-presenting cells; they can infiltrate several target organs, such as skin, liver, and the gastrointestinal tract, where they exert cytotoxic effects. This tissue-specific destruction of GVHD target organs underscores the importance of the migration capabilities of alloreactive T lymphocytes (Hill and Ferrara, 2000).

MSCs (mesenchymal stem cells) suppress alloantigen-induced T cell function *in vitro* and *in vivo* and might be a promising therapy for GVHD. In our previous study, we observed that MSCs inhibited GVHD of mice in a dose-dependent manner, and the MSCs induced activation and proliferation of regulatory T cells (Joo et al.,

2010). In particular, the *in vivo* immunosuppressive mechanisms associated with the MSCs were more closely related to the movement of infused cells after transplantation. Therefore, a new method, the measurement of the localization of infused cells in the viable state, was developed by measuring the biofluorescence of donor EGFP (enhanced green fluorescent protein) from splenocytes and RFP (red fluorescent protein) from the MSCs.

This study was designed to test the efficacy of biofluorescence imaging for tracking MSCs and splenocytes after intravenous injection in a mouse model of GVHD, to investigate their distribution over time.

2. Materials and methods

2.1. Mice

The animal care committee at the National Cancer Center (Ilsan, Gyunggi, South Korea) approved all of the procedures and protocols used in this study. Eight to twelve-week-old female C57BL/6 (H-2K^b) and BALB/c nude mice were purchased from Koatec. The EGFP-transgenic mice were obtained from RIKEN BRC (BRC No. C57BL/6-Tg (CAG-EGFP) C14-Y01-FM131Os). Transgenic C57BL/6 RFP mice were obtained from the Jackson Laboratory.

¹ To whom correspondence should be addressed (email ykh@ewha.ac.kr).

Abbreviations: BMC, bone marrow cell; DAPI, 4,6-diamidino-2-phenylindole; EGFP, enhanced green fluorescent protein; GAPDH, glyceraldehydes 3-phosphate dehydrogenase; GVHD, graft-versus-host disease; HSCT, haematopoietic stem cell transplantation; LNs, lymph nodes; MSCs, mesenchymal stem cells; RFP, red fluorescent protein; RT, real time.

2.2. Murine MSC isolation, culture expansion, and *in vitro* differentiation

MSCs were obtained from the C57BL/6 and C57BL/6 RFP mice. They were cultured as described in a previous publication (Joo et al., 2010). BMCs (bone marrow cells) were isolated and plated on 25- to 75-cm² flasks at concentrations of 5×10^6 /ml per cm² nucleated cells in complete MesenCult[®] basal medium for murine MSCs (StemCell Technologies) containing MSC stimulatory supplements, 100 units/ml penicillin and 100 µg/ml streptomycin (Invitrogen Life Technologies); they were incubated at 37°C in a 5% CO₂ in air atmosphere. Before experimental use, the MSCs were identified by the expression of CD73, CD105 and CD106 antigens but not CD45 or CD34 antigens and whether they could differentiate into lipoblasts (Jung et al., 2007; Ko et al., 2008).

2.3. Haematopoietic stem cell transplantation

Recipient female BALB/c nude mice received 5 Gy from a cesium irradiator. They were reconstituted with 5×10^6 BMCs from C57BL/6 donor mice within 24 h after irradiation of the recipient mice. To induce GVHD, 1×10^6 splenocytes from the C57BL/6 or EGFP C57BL/6 were added to the BM transplant. The treated mice received 1×10^6 MSCs from either C57BL/6 or RFP C57BL/6 (donor background) in 200 µl of complete MesenCult[®] medium. The MSCs were administered intravenously 10–15 min before the splenocytes plus BMT. The controls included irradiated mice receiving 1×10^6 spleen cells and 5×10^6 BMCs from C57BL/6 donor mice.

2.4. *In vivo* fluorescent imaging

For assessment of the spleen cells and MSCs *in vivo*, 5×10^6 C57BL/6 BMCs, 1×10^6 GFP spleen cells and 1×10^6 RFP MSCs were injected intravenously on day 0, 24 h after radiation. *In vivo* distribution of the infused splenocytes and MSCs was monitored by a live animal imaging system (IVIS 200; Xenogen), per manufacturer's directions. To control for the background photon emission, the obtained data were subjected to average background subtraction, using data from control mice that were

injected with 5×10^6 C57BL/6 BMCs and 1×10^6 C57BL/6 spleen cells. The photon radiance on the surface of an animal was expressed as photons per second per centimetre squared per steradian. Images shown are compound pictures generated by Living Image software (Figures 1, 2 and 3).

2.5. RT (real-time) PCR

RNA for reverse transcription was extracted from tissue with TRIZOL reagent (Invitrogen) according to the manufacturer's instructions. Reverse transcription was performed using the reverse transcription system (Promega). RT-PCR with relative quantification of the target gene copy number in relation to GAPDH (glyceraldehydes 3-phosphate dehydrogenase) transcripts was carried out using the following primers: EGFP forward: 5'-GCCACCATGGTGAGC-3'; reverse: 5'-TTACTTGTACAGCTCG TCC-3' and RFP forward: 5'-CCCCGTAATGCAGAAGAAGA-3'; reverse: 5'-CTTGGCCATGTAGGTGGTCT-3'. GAPDH forward: 5'-GTCTTCTCCACCATGGAGAAGGCT-3'; and reverse: 5'-CATGCC AGTGAGCTTCCCGTTCA-3'. The ABI PRISM 7000 sequence detection system (Applied Biosystems) was used to monitor RT-PCR amplification with SYBR Green (Applied Biosystems).

2.6. Confocal microscopy analysis

The frozen tissue samples were mounted in Vectashield medium containing DAPI (4,6-diamidino-2-phenylindole) (Vector Laboratories). Images were acquired by confocal microscopy on a Carl Zeiss LSM 510 META confocal microscope (Carl Zeiss) with a Plan Apochromat $\times 63$ N.A. 1.4 objective using the LSM510 software, version 3.2 (Carl Zeiss).

2.7. Immunohistochemistry for the detection of EGFP and RFP cells

At the time of sacrifice, the organs were excised and immediately placed in 10% neutral-buffered formalin. Paraffin embedded blocks were cut at 5 µm, mounted onto Superfrost/Plus slides (Fisher Scientific) and then deparaffinized in xylene and rehydrated through

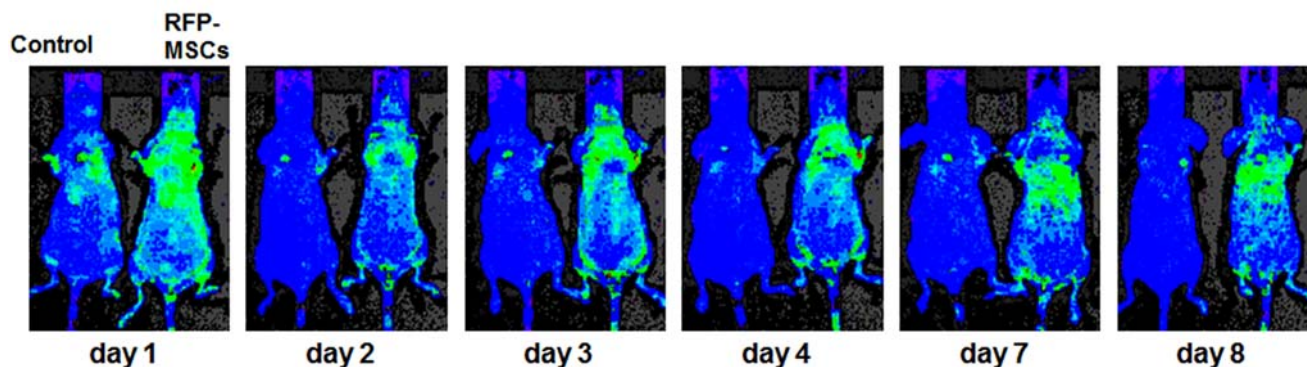


Figure 1 The fate of infused RFP-MSCs in syngeneic bone marrow transplantation
Intravenous injection in RFP-MSCs showed accumulation in the lungs, cervical LNs, stomach, liver and spleen. The left side signal represented the background. The RFP-MSCs were injected intravenously on day 0 and evaluated by optical imaging using the IVIS-Xenogen system with RFP filter according to time.

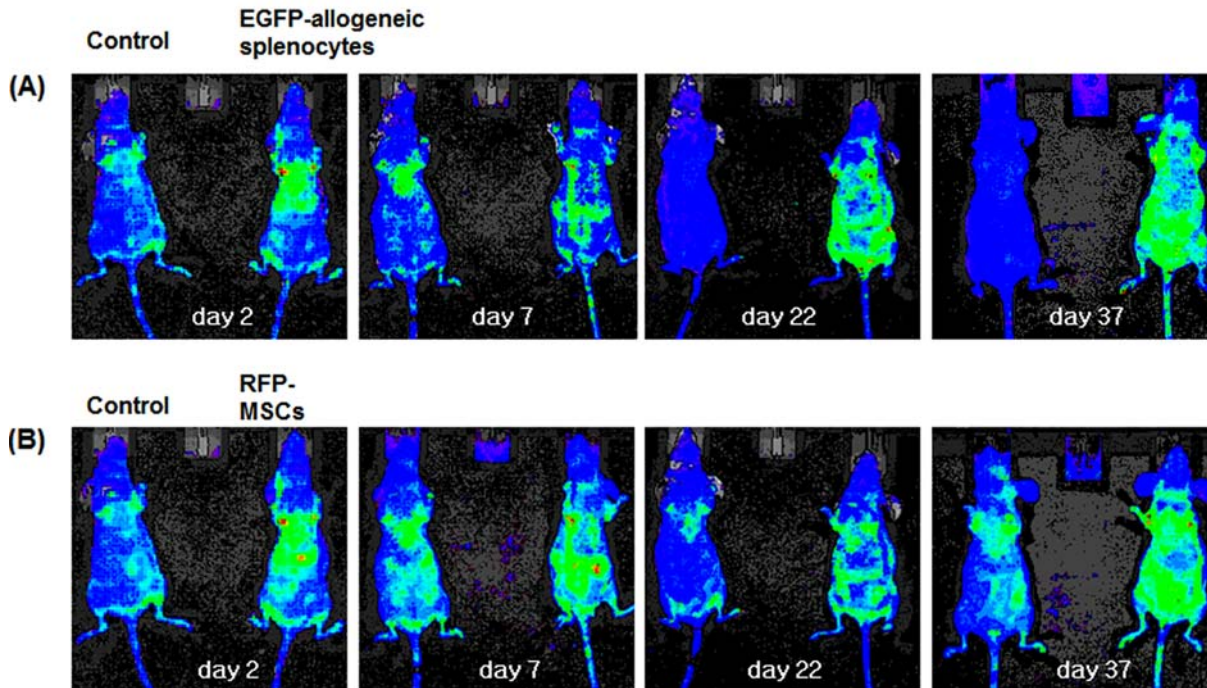


Figure 2 The fate of infused allogeneic GFP–splenocytes or RFP–MSCs
 Injected EGFP splenocytes and RFP MSCs were similar with regard to their migration fate by bioimaging; 1×10^6 EGFP spleen cells and 1×10^6 RFP–MSCs were injected by the intravenous route; EGFP (A) and RFP (B) signals were detected in the GFP and RFP filters, individually. The left side signal was evaluated as background.

an ethanol bath. Immunohistochemical staining was performed using the Ultravision LP Detection System HRP Polymer and DAB Plus Chromogen kit (Lab Vision Corporation) according to the manufacturer's protocol. Primary antibodies were mouse anti-RFP monoclonal antibodies (dilution of 1:50; BioVision) or mouse anti-EGFP monoclonal antibodies (dilution of 1:50; Chemicon International Inc.). Counterstaining was carried out with Mayer's Hematoxylin (DakoCytomation). Controls were incubated with the omission of the primary antibodies.

2.8. Statistical analysis

Data are expressed as the means \pm S.D. For the primary data collection, Excel was used (Microsoft), and the statistical analyses were carried out using Prism (GraphPad). The two-sample *t* test was used to compare the results. A *P*-value <0.05 was considered significant.

3. Results

3.1. The fate of the infused MSCs and splenocytes in the setting of GVHD

Syngeneic bone marrow transplantation with RFP–MSC signals

For monitoring the *in vivo* imaging of injected MSCs, 1×10^6 RFP–MSCs were added to the Balb/c BMC transplanted recipient mice

(donor C57BL/6, recipient Balb/c). RFP signals were detected in the lungs and cervical LNs (lymph nodes) at 3–4 days and then moved to the stomach and spleen at 7–8 days (Figure 1). These signals were always compared with the background of 1×10^6 C57BL/6 splenocytes added to the BMC-transplanted recipient mice.

3.2. Allogeneic bone marrow transplantation with GFP–splenocytes or RFP–MSC signals

For the allogeneic bone marrow transplantation conditions, to determine the *in vivo* migration of spleen cells and MSCs, these cells were infused into the C57BL/6 BMC-transplanted recipient mice (donor C57BL/6, recipient Balb/c). Two days after the infusion, the EGFP spleen cell signals were detected in the lungs (Figure 2A), and the RFP–MSC signals were very similar in appearance to the EGFP (Figure 2B). These EGFP and RFP signals moved to the oesophagus, stomach, small intestine and large intestine from the lungs together at 7 days after the infusion. The EGFP spleen cells were finally home in the axillary, inguinal and mesenteric LNs at 22–37 days, and the RFP–MSCs migrated by a similar route (Figure 2).

3.3. Co-localization of injected EGFP splenocytes and RFP–MSCs

To assess where the infused EGFP splenocytes and RFP MSCs were located *in vivo*, imaging was performed, and then, the animals were sacrificed on day 37 (Figure 3A). Homogenized

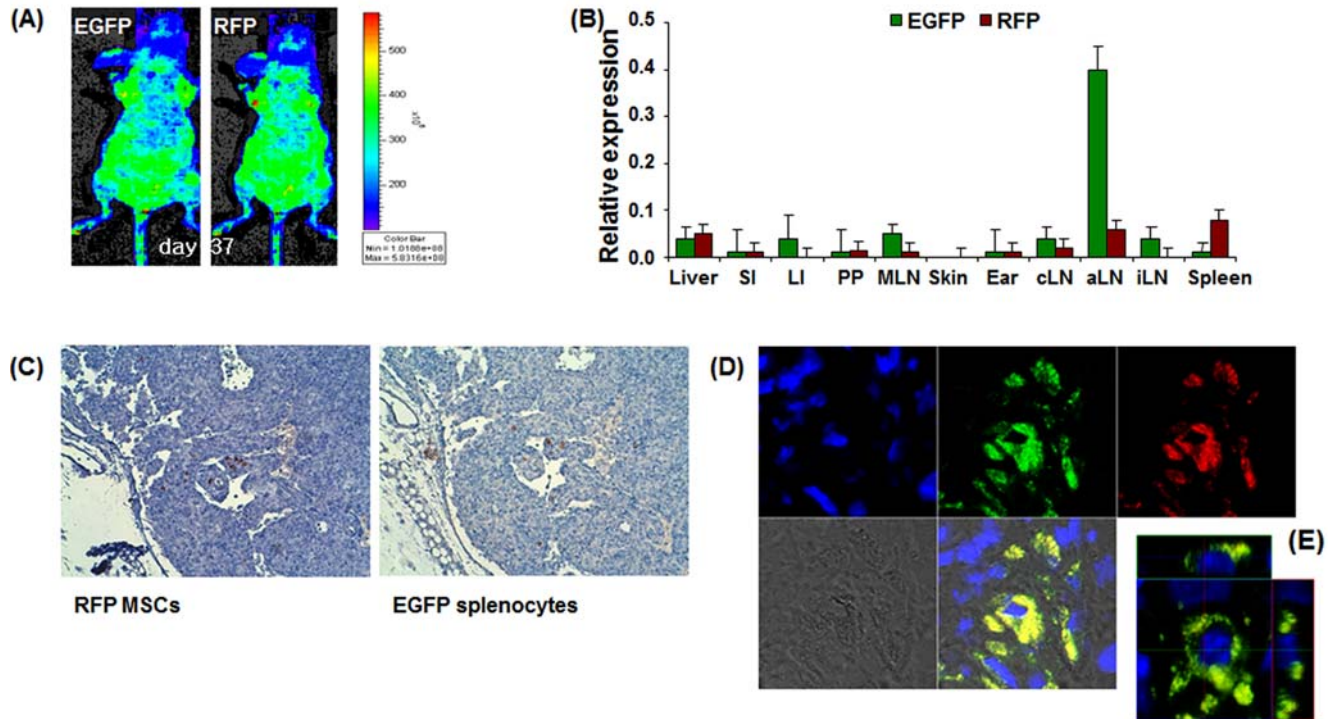


Figure 3 Colocalization of injected EGFP splenocytes and RFP-MSCs. Injected EGFP splenocytes and RFP MSCs colocalized in secondary lymphoid organs on day 37 by bioimaging with GFP (left) and RFP filter (right) (A), and confirmed by RT-PCR analysis of EGFP and RFP DNA (B). Immunohistochemical staining of a mesenteric LN with RFP (left) or EGFP (right) monoclonal antibodies (C). Confocal microscopic examination of a LN; the nucleus was visualized as blue fluorescence with DAPI (upper left); the EGFP splenocytes and RFP-MSCs are shown as green (upper middle) and red fluorescence (upper right) (D–E). They colocalized and are shown in yellow (lower middle and E).

tissues were examined by RT-PCR in different organs including the target organs of GVHD. EGFP splenocytes were mainly detected in the axilla, cervical, inguinal and mesenteric LNs, as well as the large intestine and liver. RFP-MSCs were mainly detected in the spleen, liver, axillary LNs and the cervical LNs (Figure 3B).

Serial sections of paraffin blocks were constructed for the evaluation and the colocalization of EGFP splenocytes and RFP-MSCs using monoclonal antibodies. RFP-MSCs were detected in the paracortical area, perisinusoidal area and medulla of the LNs.

EGFP splenocytes were also detected in the same areas (Figure 3C). The confocal microscopic images showed that the cytoplasm of the EGFP splenocytes and RFP-MSCs were present in green and red, respectively. They were colocalized and detected in yellow (Figures 3D–3E).

4. Discussion

The *in vivo* immunosuppressive mechanisms associated with MSCs are closely related to their movement. A new method for the measurement of localization of infused viable cells was developed that measured the biofluorescence of EGFP splenocytes and RFP MSCs.

First, the efficacy of the biofluorescence imaging for tracking the MSCs and splenocytes was tested after intravenous injection

into a mouse model of GVHD; their distribution over time was studied. Transplanted EGFP splenocytes and RFP MSCs were identified with different fluorescent filters in the bioimaging system.

For the syngeneic controls, the intravenously injected RFP-MSCs were mainly localized in the lungs. This finding is consistent with prior reports (Gao et al., 2001; Lee et al., 2009). However, in the group with GVHD, 2 days later after the infusion, the EGFP splenocyte signal was highest in the axillary LNs and detected in the lungs and stomach. The RFP-MSC signals were very similar in appearance to the EGFP splenocytes; the stomach signal was more intense than the EGFP. These EGFP splenocytes and RFP-MSC signals moved to the oesophagus, stomach, small intestine and large intestine from the lungs together on day 7 after the infusion. The EGFP splenocytes were finally home in the axillary, inguinal, mesenteric LN and ears by 22–37 days, and the RFP-MSCs migrated by a similar route. The infused cells first moved to the lungs and then the GI (gastrointestinal) tract, and finally homed to the LNs and skin. These results are consistent with the clinical manifestation of GVHD. First, the GI symptoms occur with acute GVHD, and as time goes on, the skin manifestations become the main problem.

These cells in tissues were also confirmed by RT-PCR, immunohistochemistry and confocal microscopy on day 37. Using RT-PCR analysis, the EGFP and RFP cells were confirmed to be mainly present in the regional LNs. Further identification of

the colocalization of these cells was confirmed by serial sections. They were localized in the paracortical area, perisinusoidal area and medulla of the LNs. The confocal microscopic images confirmed their colocalization. The similarity of the migration pattern and timing of the transplanted MSCs and splenocytes in the GVHD mouse model was a unique finding of this study. These data is a contradiction that MSCs may fail to efficiently reach the target tissues in GVHD (Badillo et al., 2008); thus, the likelihood of formation of the cell–cell networks and local cytokine environment that occurs *in vitro* would be minimal (Badillo et al., 2008). The results of this study demonstrated that not only soluble factors (Di Nicola et al., 2002; Rasmusson et al., 2003; Tse et al., 2003) but also cell–cell direct contact (Krampera et al., 2003; Tse et al., 2003) of the MSCs might be the mechanism associated with prevention and treatment of GVHD.

The use of this advanced optical imaging will provide innovative preclinical tools and a new platform for further improving of our understanding of the effects of GVHD. In conclusion, biofluorescence imaging was a sensitive tool that was used to demonstrate *in vivo* cell distribution and cell survival. Such investigations can substantially aid preclinical testing and the study of cell-based treatment protocols.

Author contribution

All authors participated in group discussions of the project conception and design. Sun-Young Joo drafted the manuscript. Han-seong Kim, Seong-Yeol Park, Yong-Bock Choi and Kyung-man Hong analysed and interpreted the data. Yun-Jae Jung, So-Youn Woo, Ju-Young Seoh and Kyung-Ha Ryu edited and approved the final manuscript.

Funding

This work was supported by the Korea Food and Drug Administration in 2009 [grant number 09172KFDA652]. The first author was supported by grants from the Health Fellowship Foundation and the Ewha Womans University Medical School Fellowship Foundation.

References

- Badillo AT, Peranteau WH, Heaton TE, Quinn C, Flake AW. Murine bone marrow derived stromal progenitor cells fail to prevent or treat acute graft-versus-host disease. *Br J Haematol* 2008;141:224–34.
- Blazar BR, Korngold R, Vallera DA. Recent advances in graft-versus-host disease (GVHD) prevention. *Immunol Rev* 1997;157:79–109.
- Di Nicola M, Carlo-Stella C, Magni M, Milanese M, Longoni PD, Matteucci P et al. Human bone marrow stromal cells suppress T-lymphocyte proliferation induced by cellular or nonspecific mitogenic stimuli. *Blood* 2002;99:3838–43.
- Gao J, Dennis JE, Muzic RF, Lundberg M, Caplan AI. The dynamic *in vivo* distribution of bone marrow-derived mesenchymal stem cells after infusion. *Cells Tissues Organs* 2001;169:12–20.
- Hill GR, Ferrara JL. The primacy of the gastrointestinal tract as a target organ of acute graft-versus-host disease: rationale for the use of cytokine shields in allogeneic bone marrow transplantation. *Blood* 2000;95:2754–9.
- Joo SY, Cho KA, Jung YJ, Kim HS, Park SY, Choi YB et al. Mesenchymal stromal cells inhibit graft-versus-host disease of mice in a dose-dependent manner. *Cytotherapy* 2010;12:361–70.
- Jung YJ, Ju SY, Yoo ES, Cho SJ, Cho KA, Woo SY et al. MSC–DC interactions: MSC inhibit maturation and migration of BM-derived DC. *Cytotherapy* 2007;9:451–8.
- Ko E, Cho KA, Ju SY, Woo SY. Mesenchymal stem cells inhibit the differentiation of CD4+ T cells into interleukin-17-secreting T cells. *Acta Haematol* 2008;120:165–7.
- Krampera M, Glennie S, Dyson J, Scott D, Laylor R, Simpson E et al. Bone marrow mesenchymal stem cells inhibit the response of naive and memory antigen-specific T cells to their cognate peptide. *Blood* 2003;101:3722–9.
- Lee RH, Pulin AA, Seo MJ, Kota DJ, Ylostalo J, Larson BL et al. Intravenous hMSCs improve myocardial infarction in mice because cells embolized in lung are activated to secrete the anti-inflammatory protein TSG-6. *Cell Stem Cell* 2009;5:54–63.
- Rasmusson I, Ringden O, Sundberg B, Le Blanc K. Mesenchymal stem cells inhibit the formation of cytotoxic T lymphocytes, but not activated cytotoxic T lymphocytes or natural killer cells. *Transplantation* 2003;76:1208–13.
- Thomas ED, Storb R, Clift RA, Fefer A, Johnson L, Neiman PE et al. Bone-marrow transplantation (second of two parts). *N Engl J Med* 1975;292:895–902.
- Tse WT, Pendleton JD, Beyer WM, Egalka MC, Guinan EC. Suppression of allogeneic T-cell proliferation by human marrow stromal cells: implications in transplantation. *Transplantation* 2003;75:389–97.

Received 28 July 2010/30 August 2010; accepted 9 November 2010

Published as Immediate Publication 9 November 2010, doi 10.1042/CBI20100563